

Variability in the phytoplankton community of Kavaratti reef ecosystem (northern Indian Ocean) during peak and waning periods of El Niño 2016

Kusum Komal Karati · G. Vineetha · N. V. Madhu · P. Anil · M. Dayana · B. K. Shihab · A. I. Muhsin · C. Riyas · T. V. Raveendran

Received: 7 June 2017 / Accepted: 15 November 2017 / Published online: 29 November 2017
© Springer International Publishing AG, part of Springer Nature 2017

Abstract El Niño, an interannual climate event characterized by elevated oceanic temperature, is a prime threat for coral reef ecosystems worldwide, owing to their thermal threshold sensitivity. Phytoplankton plays a crucial role in the sustenance of reef trophodynamics. The cell size of the phytoplankton forms the “master morphological trait” with implications for growth, resource acquisition, and adaptability to nutrients. In the context of a strong El Niño prediction for 2015–2016, the present study was undertaken to evaluate the variations in the size-structured phytoplankton of Kavaratti reef waters, a major coral atoll along the southeast coast of India. The present study witnessed a remarkable change in the physicochemical environment of the reef water and massive coral bleaching with the progression of El Niño 2015–2016 from its peak to waning phase.

Electronic supplementary material The online version of this article (<https://doi.org/10.1007/s10661-017-6369-5>) contains supplementary material, which is available to authorized users.

K. K. Karati (✉) · G. Vineetha · N. V. Madhu · P. Anil · M. Dayana · T. V. Raveendran
National Institute of Oceanography-CSIR, Dr. Salim Ali Road, Kochi, India
e-mail: kusum111@gmail.com
e-mail: karatik@nio.org

B. K. Shihab · A. I. Muhsin · C. Riyas
Department of Science and Technology, Kavaratti, Lakshadweep, India

Present Address:
G. Vineetha
Central Marine Fisheries Research Institute, Kochi, India

The fluctuations observed in sea surface temperature, pH, and nutrient concentration of the reef water with the El Niño progression resulted in a remarkable shift in phytoplankton size structure, abundance, and community composition of the reef waters. Though low nutrient concentration of the waning phase resulted in lower phytoplankton biomass and abundance, the diazotroph *Trichodesmium erythraeum* predominated the reef waters, owing to its capability of the atmospheric nitrogen fixation and dissolved organic phosphate utilization.

Keywords El Niño · Reef ecosystem · Nutrient · Phytoplankton · Size structure

Introduction

Coral reefs are one among the most biodiverse and productive ecosystems in the marine realm and are considered analogous to “tropical rainforests” (Spalding et al. 2001). Coral reefs are also remarkable for their valuable socioeconomic and ecological services in terms of fisheries, coastal protection, tourism, and as a source of potential pharmaceuticals (Carte 1996; Cinner et al. 2012). Reef ecosystems are extremely fragile regions, vulnerable to perturbations induced by both natural and anthropogenic origins (Hughes et al. 2003). The corals that play a fundamental role in the reef ecosystem often live close to their thermal thresholds (Baker et al. 2008). Henceforth, any subtle variations in their physicochemical environment, especially in the temperature, can be highly detrimental to their

health and survival. Of the many natural threats, the rising sea surface temperature (SST) associated with global warming and interannual climate events like El Niño have been reported to cause severe and extensive impacts on the coral reef ecosystems worldwide (Normile 2016). The El Niño–Southern Oscillation (ENSO), a coupled ocean-atmospheric climatic phenomenon originating in the eastern and central Pacific Ocean, contributes immensely to the fluctuations in the normal weather pattern worldwide and most significantly in the tropical and subtropical regions (McPhaden et al. 2006). The warm oceanic episode of the ENSO cycle, the El Niño, characterized by higher SST than normal over central and eastern equatorial Pacific are known to have a profound influence on the climatology of the tropical Indian Ocean by generating fluctuations in the surface water temperature (SST) and monsoonal rainfall (Roxy et al. 2011; Gadgil and Francis 2016). The Indian subcontinent is characterized by relatively less reef area compared to other regions in the world (Venkataraman 2011). Of the prominent reef zones along the Indian coast, the Lakshadweep archipelago located 200–400 km off the south-west coast of India is well recognized for the offshore atoll reef ecosystems it harbors (Pillai 1996). Compared to the open ocean, the repercussions of climatic events like El Niño will be more intense in the shallow reef ecosystems due to the low adaptive capacity and vulnerability of corals to thermal stress and even mild variations occurring in their acclimatized physicochemical environment (Hughes et al. 2003). In coral reef ecosystems, the reef-building scleractinian corals form the fundamental structural community whose growth and vigor often forms the primary determinant shaping the abundance and community structure of the reef-associated fauna (Arthur 2000). Hence, a periodic monitoring of the status of the physicochemical environment, corals, and associated biota of reef ecosystem in the course of the El Niño climatic event is essential for the effective management and restoration of this vulnerable yet valuable ecosystem in the tropical Indian Ocean.

Phytoplankton occupies an important ecological niche in the reef ecosystems (Racault et al. 2015). As the biomass and phenology of phytoplankton have a significant role in determining the trophic interactions, they are often taken as suitable ecological indicators for the changes associated with environmental perturbations from both natural and anthropogenic causes (Bell and Elmetri 1995). Similar to the reef-building corals,

the responses of phytoplankton taxa to temperature vary widely (Canale and Vogel 1974). As temperature has a prime role in determining the growth, photosynthetic rate, nutrient stoichiometry, and distribution of the phytoplankton, the unprecedented increase in the SST associated with climatic variability like El Niño are expected to have a significant effect on their phenology and community structure (Garate-Lizarraga and Beltrones 1998). Besides temperature, the concentration and stoichiometry of the nutrients, especially nitrogen (both new and regenerated) and phosphorus, often have a decisive role in determining the ecology and size distribution of the phytoplankton community (Guildford and Hecky 2000; Sommer 2000). Hence, a critical analysis of the size structure of phytoplankton standing stock is often used to elucidate the variability in the trophodynamics of ecosystems (Maranón et al. 2012). However, the responses of the different phytoplankton size categories to interannual climatic events like El Niño are least studied (Furnas 2007). The present study throwing light on the standing stock and ecology of the size-structured phytoplankton community during the interannual climatic event El Niño will be beneficial in unraveling the responses of the phytoplankton community in similar shallow reef ecosystems in the tropical and subtropical belts.

The high-average SST initiated by the westerly wind bursts over the equatorial western Pacific during late 2015 to early 2016 brought about intense weather fluctuations around the globe and is henceforth depicted as the El Niño 2015–2016 event or the “Godzilla El Niño” (Stramma et al. 2016). The current El Niño is considered as one of the strongest events since 1950 (Chen et al. 2016) and is expected to have a perilous impact on the reef community worldwide, resulting in mass coral bleaching and mortality events. Taking into consideration, the impacts caused by the El Niño 1998 affecting more than 80% of the corals in the Lakshadweep reef ecosystem (Arthur 2000), and the void in the knowledge on the responses of the size-structured phytoplankton community of the Lakshadweep reef atoll, the present study was designed to understand (a) the changes occurring in the physical environment of reef waters and live corals in course of the El Niño climatic event and (b) the nutrient dynamics of reef waters during the El Niño evolution and its subsequent effect on the phytoplankton standing stock and community structure.

Materials and methods

Study area

The Lakshadweep archipelago (8–12°N and 71–74°E), comprising of 12 atolls, 3 reefs, and 5 submerged banks located in the southeastern Arabian Sea, northern Indian Ocean, forms an ecologically significant and unique region being the only offshore reef ecosystem along the Indian coast (James 2011). These offshore atolls, though located amidst the oligotrophic oceanic waters, are remarkable for their high biodiversity and biological productivity (Suresh and Mathew 1999). Kavaratti atoll forms one of the largest and prominent atolls in the Lakshadweep archipelago. Being oriented in the north-south direction, it has a shallow lagoon (average depth 2 m) enclosed by a reef on the west, an island in the east, and is about 4500 m in length and 1200 m in width. Though the reef-building corals form the predominant community in Kavaratti atoll, the reefs also support diverse ecologically relevant flora and fauna, including seagrass and turtles (Pillai and Jasmine 1989).

Sampling

For the present study, sampling was carried out at 10 locations covering the entire Kavaratti lagoon in a north-south direction. The sampling sites included both landward and seaward locations of the lagoon (Fig. 1). As the prime aim of the study was to understand the impact of El Niño on the phytoplankton community of the reef waters, the sampling period was priori designed based on the El Niño forecast acquired from the Earth Institute, Colorado University (<http://iri.columbia.edu/ouexpertize/climate/forecasts/enso/2016>). Based on the forecast, the first sampling was carried out during the peak period of El Niño (first week of March 2016). The subsequent sampling was done after a time gap of ~80 days, when the El Niño was in its waning phase (last week of May 2016). To affirm the influence of this climatic event on the SST distribution around the Lakshadweep archipelago, the satellite-generated SST data of the Lakshadweep Sea, in the vicinity of the coral atolls (8–12°N and 71–74°E), was analyzed. To get a precise picture of the surface temperature of the region, the satellite SST data for the period of 2010–2016, the last ENSO cycle (strong La Niña—2010 to 2011, neutral—2012 to early 2015, strong El Niño—late 2015 to early 2016), was verified

(<http://ggweather.com/enso/oni.htm>). The monthly mean SST was extracted based on GAC in NOAA Ocean Watch LAS (June 2010–December 2015) and MODISA_L3m_SST (January–May 2016). Rainfall pattern in and around the Lakshadweep Sea region was described based on the monthly data of Indian Meteorological Department, Trivandrum (<http://www.imdtvm.gov.in>).

Water samples for the analysis of the physicochemical variables and phytoplankton (biomass and composition) were collected using a Niskin sampler (5-L capacity). The temperature was measured using a bucket thermometer. For determining the salinity of the surface water, water samples were analyzed in an Autosol (DIGI-AUTO Model-5) with precision ± 0.005 psu. pH was measured using a calibrated pH meter (ELICO LI610, accuracy ± 0.01). The nutrient concentration of the water samples (dissolved inorganic nitrate-N, nitrite-N, ammonia-N, phosphate-P, and silicate-Si) were determined using an auto-analyzer (SKALAR San++ System, Netherlands).

The size-fractionated phytoplankton standing stock (chlorophyll *a*) from each sampling location was analyzed by sequentially filtering 2 L of the surface water samples. Initially, the water samples were passed through a 200- and 20- μ m mesh, respectively. The phytoplankton cells entrained in the 200- μ m mesh formed the macroplankton, whereas those retained by the 20- μ m mesh belonged to the microplankton size category. Following the filtration, the respective meshes were reverse washed with distilled water and were subsequently passed through glass fiber filters (GF/F; nominal pore size 0.7 μ m) to determine the pigment concentration corresponding to the respective size classes. The filtered water samples were again successively passed through 2- and 0.2- μ m polycarbonate filters for estimating the nanoplankton and picoplankton biomass, respectively. Subsequent to the filtration process, the pigments of the respective size groups of phytoplankton were extracted in 90% acetone for 24 h in the dark at 4 °C, and the pigment concentration was estimated using Turner's fluorometer (Turner Designs, 7200). For the qualitative and quantitative analysis of the phytoplankton community, 2 L of surface water collected was preserved immediately using 1% acid Lugol's iodine solution. After the settling and siphoning procedure (Utermöhl 1931) in the laboratory, 1 mL of aliquots of samples was taken in a Sedgewick-Rafter counting cell and the phytoplankton cells were correspondingly

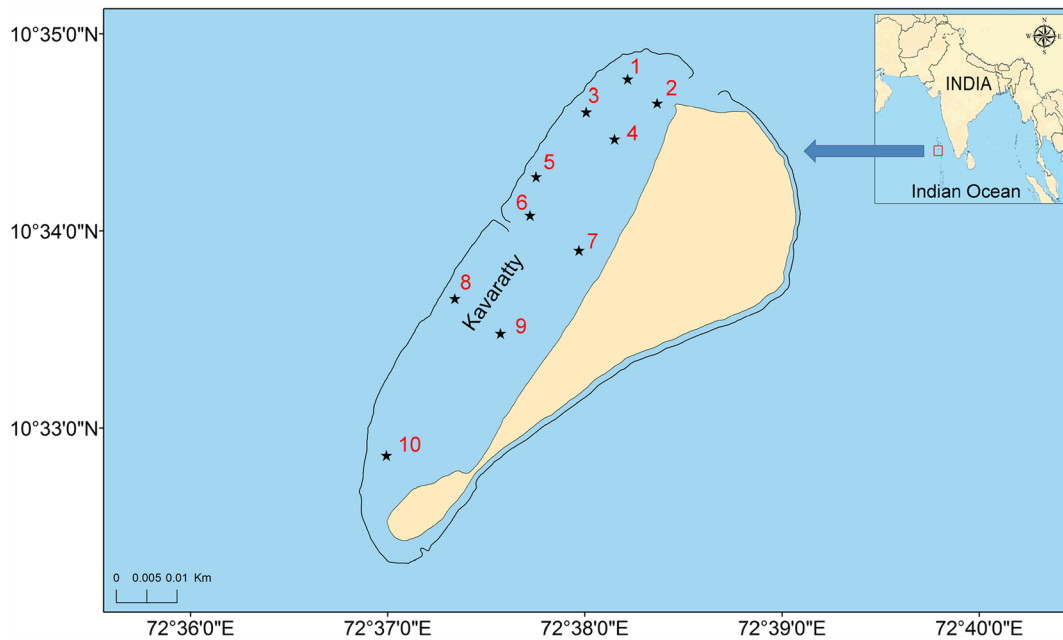


Fig. 1 Distribution of station location in the Kavaratti lagoon in the Lakshadweep Sea

identified and enumerated under an inverted binocular microscope (OLYMPUS, CK-30, magnification $\times 100$) following the standard protocols (Tomas 1997).

To assess the status of the corals and the coral percentage cover in the lagoon, the line intercept transect (LIT) method was carried out during October 2015 and May 2016 (English et al. 1997). The transects were laid horizontally along the substratum, and the status of the reef coral was evaluated along each transect. The taxonomic identification of the corals was done following the Indo-Pacific Coral Guide (Kelley 2009). The percentage of the coral cover in the Kavaratti atoll was monitored by snorkeling and scuba diving.

Data analyses

t test

A paired *t* test (with two-tailed *P* values and 95% confidence intervals) was performed on the datasets of the abiotic variables of the two sampling periods to have a better understanding of the significance of variation existing between the two periods. Prior to the analysis, the datasets were checked for their normality in the distribution using D' Agostino and Pearson omnibus normality test. In accordance with the normality test result, a parametric *t* test was chosen for the variables exhibiting a Gaussian distribution while a non-

parametric *t* test was done on the variables having non-Gaussian distribution. Similar to the abiotic variables, the paired *t* test analysis was also performed on the size-fractioned phytoplankton biomass (for each size fraction) and abundance of the sampling periods to assess the significance of variation existing among them.

Community indices and non-metric multidimensional analysis

To understand the variation existing in the phytoplankton assemblages of both the sampling periods, the species diversity (*H'*) and evenness (*J'*) were analyzed using the PRIMER version 7 (Clarke and Gorley 2015). Non-metric multidimensional scaling (NMDS) was performed on the fourth-root-transformed phytoplankton abundance data to interpret the distinctness in the phytoplankton community structure of the two sampling periods. The NMDS analysis was done based on the Bray-Curtis similarity index.

Multivariate dispersion analysis and analysis of similarities

The multivariate dispersion (MVDISP) algorithm was used to assess the variability in the phytoplankton community structure of the two sampling phases and to

calculate the index of multivariate dispersion (IMD). In addition, to describe the (dis)-similarities of the phytoplankton community between the two periods, the analysis of similarity (one-way ANOSIM) was done on the phytoplankton abundance data using PRIMER 7 (Clarke and Gorley 2015).

Similarity percentage routine

The characterizing species of each sampling period were identified using similarity percentage routine (SIMPER) analysis described in PRIMER. The abundance data was fourth root-transformed before the analysis. The discriminating species contributing to the dissimilarity in the phytoplankton community between the sampling periods were also identified.

Redundancy analysis

Redundancy analysis (RDA) was carried out to elucidate the relationship between the abiotic and biotic variables during two sampling periods and to identify the factors favoring the distribution of different size categories of the phytoplankton community. For this, the abiotic variables selected included temperature, salinity, pH, suspended particulate matter, and nutrients, while for the biotic variables, the biomass of different phytoplankton size categories, total phytoplankton biomass (chlorophyll *a*), and phytoplankton abundance were chosen.

Results

Environmental variables

The satellite-retrieved monthly averaged SST of the Lakshadweep Sea contiguous to the archipelago for the period of 2010–2016 exhibited a pronounced variability (Fig. 2). During the strong La Niña period of 2010–2011, the winter SST (November–February) was relatively lower compared to all the other years (2012–2016; Fig. 2). In contrast, during the El Niño period (2015–2016), the SST was higher throughout the year, thus indicating the influence of this coupled ocean-atmosphere phenomenon in this part of the northern Indian Ocean (Fig. 2). The elevated SST of the El Niño event was most evident from the middle of 2015 (July) onward. A pronounced variation in the SST was noticeable even during the waning phase of the El

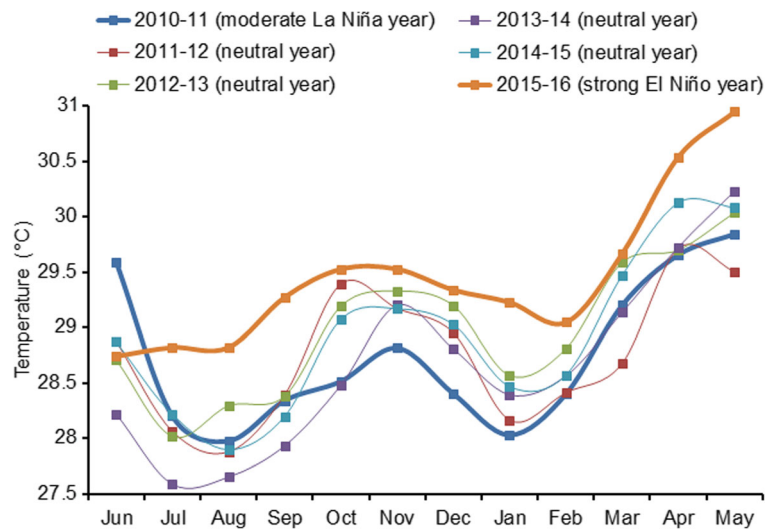
Niño (May 2016; Fig. 2). In the case of the in situ observation, the SST inside the lagoon exhibited negligible spatial variation during the peak phase (first week of March 2016; winter monsoon) and ranged from 30 to 31.4 °C (average 30.6 ± 0.5 °C) (Fig. 3a). In the waning phase of the El Niño (fourth week of May 2016; late spring intermonsoon), the in situ SST of the lagoon varied between 30.6 and 31.7 °C with an average of 31.1 ± 0.4 °C. Similar to the satellite data, most of the sampling locations inside the lagoon experienced relatively high SST during the waning phase compared to the peak period. The variation in the SST distribution between the two sampling periods was found to be statistically significant ($P < 0.05$).

A marginal variation was evident in the spatial distribution of the sea surface salinity during both the sampling periods (Fig. 3b). However, during the El Niño peak phase, the surface salinity (average 34.53 ± 0.09 , range 34.4–34.7) was slightly lower than that of the waning phase (average 34.79 ± 0.03 , range 34.7–34.8), and this variation was found to be statistically significant ($P < 0.05$). The pH of the surface water samples varied greatly between the two sampling periods (Fig. 3c). In the peak phase, the pH of the study region ranged between 7.85 and 8.05 (average 7.96 ± 0.07). During the waning phase, relatively high pH (average 8.17 ± 0.09) was observed in all the sampling locations (range 7.96–8.28).

Nutrients

Irrespective of the sampling periods, the study region was oligotrophic with low nutrient concentrations (Fig. 4). However, among the two sampling periods, the concentration of all the major nutrients (nitrite-N, nitrate-N, phosphate-P, and silicate-Si) was lower in the waning phase, resulting in a statistically significant variation between the two periods ($P < 0.05$) (Fig. 4). In general, the nitrate-N distribution exhibited marked variation with a relatively high concentration in the peak phase (average 0.46 ± 0.52 μM, range 0.01–1.8 μM) compared to the waning phase (average 0.16 ± 0.13 μM, range 0.02–0.4 μM) (Fig. 4a). The nitrite-N concentration in the study region ranged between 0.11 and 0.32 μM in during the peak El Niño period (average 0.22 ± 0.06 μM) and subsequently dropped in the waning phase (0.09 ± 0.03 μM) (Fig. 4b). Likewise, the concentration of phosphate-P during the peak El Niño phase (0.26 ± 0.15 μM) was two times higher than that observed during the waning period (0.13 ± 0.3 μM) (Fig. 4c). The silicate-Si levels during the peak

Fig. 2 Satellite-based monthly averaged SST data of the Lakshadweep Sea, in the vicinity of the coral atolls (8–12°N and 71–74°E) during the period of 2010–2016



El Niño period ranged between 3.7 and 6.3 μM (average $4.7 \pm 0.8 \mu\text{M}$), and was three times higher than the waning phase (average $1.59 \pm 0.2 \mu\text{M}$, range 1.46–1.96 μM) (Fig. 4d). However, compared to the other nutrients, the concentration of ammonia-N was relatively higher during both the sampling periods (average 8.7 ± 1 and $5.4 \pm 0.4 \mu\text{M}$, during peak and waning phases, respectively) (Fig. 4e).

Coral health

A mass bleaching was observed in the coral community of the Kavaratti atoll during the El Niño event. During May 2016, bleaching of about 60% of the corals occurred in the Kavaratti atoll with severe impacts on both fast-

growing (*Acropora* sp.) and slow-growing (*Porites* sp.) massive hermatypic corals.

A conspicuous variability was also observed in the percentage of both live and dead coral cover in the atoll. During the pre-bleaching period (October 2015), the live coral contributed to 21.34%, whereas the dead coral constituted 45.96% of the total lagoon. After the El Niño 2015–2016 and the associated bleaching event, the live coral cover dropped considerably to 9.89%, and the contribution of the dead and near-dead coral increased to 57.3% (50.7% dead + 6.6% pale colored weak) in the entire lagoon. A total of 23 genera of corals were recorded in the Kavaratti atoll among which the most dominant genera in the line intercept transect were *Porites* sp.

Fig. 3 Distribution of a temperature (°C), b salinity, and c pH at the surface water of Kavaratti lagoon during the peak and waning phases of El Niño

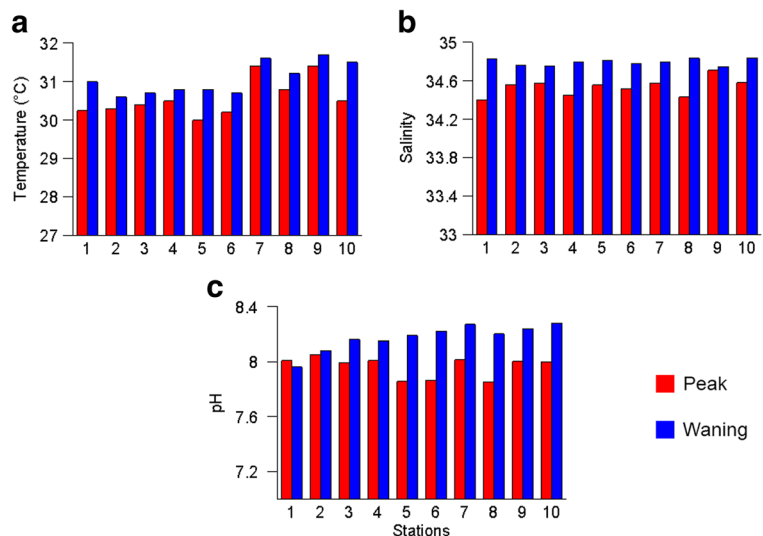
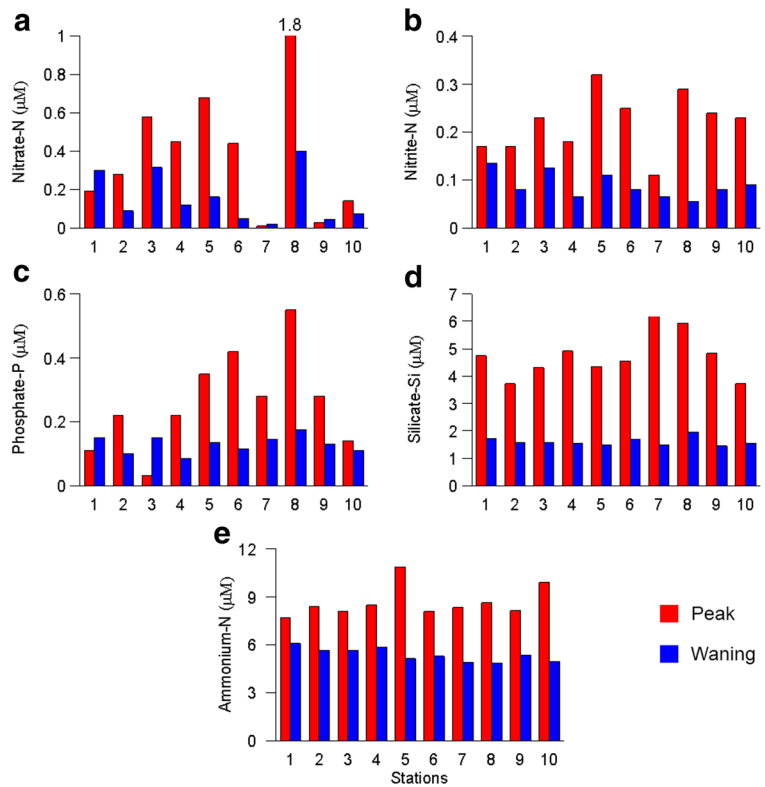


Fig. 4 Distribution of nutrients at the surface water of Kavaratti lagoon during the peak and waning phases of El Niño



(22.41%), followed by *Pocillopora* and *Oulophyllia* (Table 1).

Phytoplankton biomass

Phytoplankton biomass, represented as chlorophyll *a* concentration, exhibited pronounced spatial and temporal variations in the study region. During the peak El Niño phase, total chlorophyll *a* ranged from 0.06 and 0.43 mg m⁻³ (average 0.17 ± 0.11 mg m⁻³) (Fig. 5a). In the corresponding waning phase, it was lower in the entire study region (average 0.095 ± 0.04 mg m⁻³, range 0.06–0.19 mg m⁻³), resulting in a significant statistical variation between the two sampling periods (*P* < 0.05).

A remarkable spatial and temporal variation was evident in the relative contribution of different size categories of phytoplankton to the total biomass (Fig. 6). In general, the nanophytoplankton contributed a major share of the total biomass during both sampling periods with 69.9% contribution in the peak El Niño phase and about 57.2% in the waning period (Fig. 6). Furthermore, the pigment concentration of the nanophytoplankton community during the peak phase (average 0.12 ± 0.07 mg m⁻³) was about 2.2 times higher than that observed during the

waning phase (average 0.055 ± 0.03 mg m⁻³). Besides nanophytoplankton, the microphytoplankton also contributed a significant share of the total chlorophyll *a*, sharing a 16.6% in the peak phase and 21.5% in the waning phase. The microphytoplankton biomass was also higher during the peak phase (average 0.035 ± 0.05 mg m⁻³) than the waning phase (average 0.019 ± 0.006). In comparison with the other size categories, the macrophytoplankton biomass was markedly higher in the waning phase (0.01 ± 0.01 mg m⁻³, 8.4% of the total chlorophyll *a*) compared to the peak phase (average 0.002 ± 0.004 mg m⁻³, 2.9% of the total chlorophyll *a*). Though the percentage contribution of the small-sized picophytoplankton did not vary much between the two sampling periods (10.6 and 12.4%, in the peak and waning phases, respectively), their pigment concentration was 1.4 times higher in the peak phase (0.014 ± 0.012 mg m⁻³) compared to the waning phase (0.01 ± 0.01 mg m⁻³).

Phytoplankton abundance and composition

Similar to chlorophyll *a*, phytoplankton abundance also exhibited pronounced spatial and temporal variability between the two sampling periods (Fig. 5b). Abundance

Table 1 The coral community in the Kavaratti atoll (+ indicates $\leq 1\%$, ++ indicates $>1-5\%$, +++ indicates $>5-10\%$, ++++ indicates $>10-20\%$, +++++ indicates $>20\%$)

Genus	Contribution
<i>Acropora</i>	++
<i>Montipora</i>	++
<i>Astreopora</i>	+
<i>Fungia</i>	+
<i>Cyphastrea</i>	+
<i>Favites</i>	+
<i>Favia</i>	++
<i>Galaxea</i>	+
<i>Gardineroseris</i>	+
<i>Goniastrea</i>	++
<i>Hydnophora</i>	++
<i>Leptastrea</i>	++
<i>Oulophyllia</i>	++++
<i>Lobophyllia</i>	+++
<i>Pachyseris</i>	+
<i>Pavona</i>	+++
<i>Platygyra</i>	++
<i>Plesiastrea</i>	+
<i>Pocillopora</i>	++++
<i>Porites</i>	+++++
<i>Psammocora</i>	++
<i>Symphyllia</i>	++
<i>Trachyphyllia</i>	+

during the peak phase (3968 ± 2540 cells L^{-1}) was about 2.8 times higher than that observed during the waning phase (1408 ± 802 cells L^{-1}), thus resulting in a statistically significant variation ($P < 0.05$).

The relative contribution of the different phytoplankton functional groups toward the total phytoplankton community also showed a prominent

variability between the two sampling periods. During the peak phase, dinoflagellates (56.5%) formed the dominant taxa, followed by the diatoms (36.3%). However, the higher contribution of the dinoflagellates mostly resulted from an exceptionally higher abundance of the dinoflagellate species, *Prorocentrum lima*, in two sampling locations 7 and 9 ($>80\%$). In the waning period of El Niño, diatoms formed the dominant taxa (54.5%). A noteworthy feature observed during the study was the relatively high contribution of the cyanobacterial population to the phytoplankton abundance in the waning phase of the El Niño event (33.2%). Dinoflagellates, the dominant taxa in the peak phase, were observed to have a lesser contribution to the phytoplankton community during this period (8.2%). Of the 36 phytoplankton species observed during the present study, only 15 species were found to be common for both the sampling periods (Table 2). Based on the dominancy analysis, two diatoms (*Thalassiosira* sp. and *Diploneis* sp.) and the two dinoflagellates (*P. lima* and *Protopteridinium* sp.) were identified as the dominant phytoplankton species during the peak phase. In the waning phase, diatoms, *Navicula delicatula* (24.4%) and *Licmophora abbreviata* (9.7%), formed the dominant species among the diatom community. A noticeable feature observed during the waning phase was the predominance of the cyanobacterium, *Trichodesmium erythraeum*, in all the sampling locations. They occurred both as individual trichomes and as colonies with size >200 μm (Supplementary Fig. 1). Though it contributed only a minor share of the total phytoplankton population in the peak phase, *T. erythraeum* formed one of the predominant species sharing 33.2% of the entire population in the waning phase (average 468 ± 402 cells L^{-1}) with a conspicuous higher abundance at sampling sites 7 and 10.

Fig. 5 Distribution of total chlorophyll *a* ($mg\ m^{-3}$) and phytoplankton abundance (cells L^{-1}) at the surface water of Kavaratti lagoon during the peak (red color) and waning phase (blue color) of El Niño

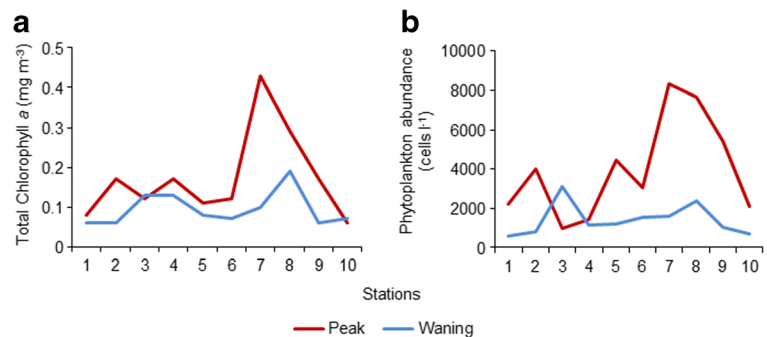
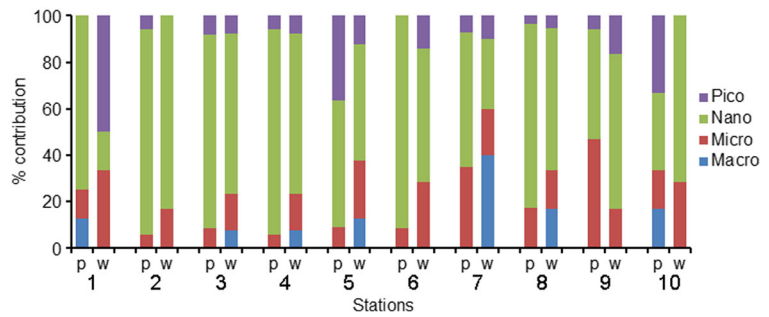


Fig. 6 The contribution of different size categories of phytoplankton to the total chlorophyll *a* at the surface water of Kavaratti lagoon (*p* peak phase, *w* waning phase)



Data analysis

Community indices

Phytoplankton species diversity (*H'*) during the peak phase varied between 1 and 3.05 with an average of 2.03 ± 0.07 (Fig. 7a). The *H'* during the waning phase was found to range between 0.59 and 3.33 with an average of 2.18 ± 0.71 . Though there was an obvious variation in the phytoplankton abundance between two sampling periods, in the case of *H'*, the difference was not significant ($P > 0.05$) (Fig. 7a). Phytoplankton species evenness (*J'*) also did not show much variation between the two sampling periods (0.86 ± 0.16 and 0.8 ± 0.17 , during peak and waning phases, respectively) and the variation was statistically insignificant ($P > 0.05$) (Fig. 7b).

NMDS

The NMDS plot based on the fourth-root-transformed phytoplankton abundance depicts the difference in the position of the sampling locations of the two sampling periods. Most of the sampling locations during the peak and waning phases were found to be ordinated separately (stress 0.17) (Supplementary Fig. 2).

Multivariate analyses

The variability observed in the phytoplankton community structure between the peak and waning phases was further probed using the MVDISP algorithm. During the peak phase, the variability in the sampling locations was found to be higher (dispersion factor value 1.226), compared to that during the waning period (dispersion factor value 0.774). The IMD was found to be 0.458 in the pairwise comparisons of the sampling sites between the peak and waning periods. In the case of the one-way

ANOSIM analysis, the phytoplankton community in the peak phase was observed to be significantly distinguishable from the community during the waning phase (global $R = 0.329$, $P = 0.002$).

SIMPER analysis

Based on the SIMPER analysis, the average similarity observed for the phytoplankton species was relatively higher during the peak (41.9) compared to the waning phase (29.9) (Tables 3 and 4). *Diploneis* sp. and *P. lima* were identified as the characterizing species of the peak phase, whereas, *T. erythraeum*, *N. delicatula*, and *L. abbreviata* formed the characterizing species in the waning phase. The average dissimilarity of the phytoplankton community between the peak and waning phases was observed to be high (72.9) (Tables 3 and 4). A total of eight species of phytoplankton (*P. lima*, *N. delicatula*, *T. erythraeum*, *Diploneis* sp., *Thalassiosira* sp., *Protoperidinium* sp., *L. abbreviata*, and *Diplopsalis* sp.) were observed to play an important role in discriminating the community structure of the two sampling periods (Tables 3 and 4).

Redundancy analysis

The RDA triplots helped in unraveling the preferred abiotic environment of the size-fractionated phytoplankton and phytoplankton abundance during both sampling periods (Fig. 8). During both phases, the biomass of the dominant nanoplankton was positively correlated with the nutrients such as nitrate-N, phosphate-P, and silicate-Si (Fig. 8). The microplankton exhibited a strong positive relation to phosphate-P, silicate-Si, and temperature than that with nitrate-N during the peak phase, whereas in the waning phase, it showed a positive correlation to the nitrate-N also (Fig. 8). In the waning phase, the macrofraction was positively correlated with

Table 2 Phytoplankton abundance (cells L⁻¹) during the peak and waning phases (* indicates ≤10 cells L⁻¹, ** indicates >10–40 cells L⁻¹, *** indicates >40–100 cells L⁻¹, **** indicates >100–400 cells L⁻¹, ***** indicates >400 cells L⁻¹)

Species	Peak	Waning
<i>Thalassiosira</i> sp.	****	**
<i>Thalassiosira subtilis</i>	**	—
<i>Leptocylindrus danicus</i>	—	**
<i>Bacteriastrium furcatum</i>	—	*
<i>Chaetoceros</i> sp.	—	*
<i>Odontella mobiliensis</i>	****	*
<i>Fragilaria crotonensis</i>	***	*
<i>Asterionellopsis glacialis</i>	—	*
<i>Pleurosigma</i> sp.	***	**
<i>Pleurosigma normanii</i>	—	*
<i>Pleurosigma elongatum</i>	—	**
<i>Gyrosigma</i> sp.	**	**
<i>Diploneis</i> sp.	****	***
<i>Diploneis smithii</i>	***	—
<i>Diploneis didyma</i>	**	—
<i>Diploneis puella</i>	**	—
<i>Navicula</i> sp.	**	**
<i>Navicula delicatula</i>	****	****
<i>Mastogloia</i> sp.	**	*
<i>Mastogloia linearis</i>	**	—
<i>Entemoneis</i> sp.	—	*
<i>Amphora obtusa</i>	**	—
<i>Licmophora abbreviata</i>	***	****
<i>Cylindrotheca closterium</i>	—	**
<i>Surirella fastuosa</i>	—	*
<i>Paralia sulcata</i>	—	*
<i>Prorocentrum lima</i>	*****	**
<i>Prorocentrum rhathymum</i>	**	—
<i>Prorocentrum compressum</i>	*****	*
<i>Gyrodinium</i> sp.	***	—
<i>Ceratium declinatum</i>	**	—
<i>Diplopsalis</i> sp.	****	**
<i>Protoperidinium</i> sp.	****	***
<i>Protoperidinium quinquecorne</i>	***	—
<i>Trichodesmium erythraeum</i>	***	*****
<i>Dictyocha fibula</i>	—	*

phosphate-P and temperature. During both the sampling periods, the picofraction was positively correlated with ammonia-N but had a negative relation with pH (Fig. 8). In case of the total phytoplankton biomass, a positive

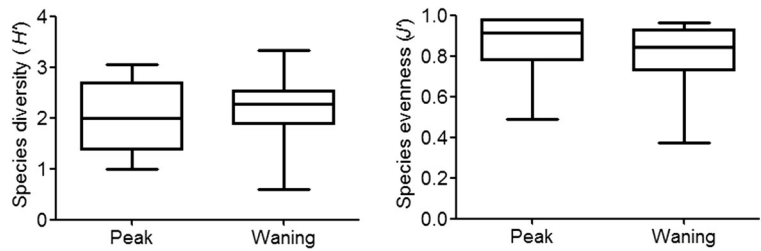
relation was observed with phosphate-P, silicate-Si, and temperature in the peak El Niño period, whereas in the waning phase, it was strongly correlated with phosphate-P (Fig. 8).

Discussion

The interannual climatic event El Niño, characterized by high SST in the equatorial Pacific Ocean, have a profound influence on the global weather patterns, but more intense in regions bordering the tropical and subtropical belts (McPhaden et al. 2006). El Niño is reported to have a prominent effect on the climatology of the northern Indian Ocean, though the severity of its impacts may vary depending on the intensity, the nature of its origin (east Pacific or central Pacific), and its interaction with the Indian Ocean dipole and the equatorial Indian Ocean oscillation (Roxy et al. 2011). The current El Niño is considered as one of the strongest since 1950 (http://www.wmo.int/pages/index_en.html). The persistently higher SST observed during 2015–2016 in this part of the Indian Ocean in concurrence with the El Niño affirms the impact of this phenomenon on the climatology and weather patterns on a global scale. However, the satellite-retrieved SST of the study region was relatively lower during the peak phase of El Niño compared to the waning period (Fig. 2). Generally, in the tropical northern Indian Ocean, the observed SST is much lower during the winter monsoon (February–March) compared to the late intermonsoon period (May) (Shenoi et al. 1999). Thus, the relatively lower SST in this part of the northern Indian Ocean during the peak El Niño phase can be attributed to this seasonal interference on the SST distribution. Similar scenario in the in situ observation of surface water temperature of the reef ecosystem with relatively higher values during the waning phase (last week of May) compared to the peak period (first week of March) further upholds the seasonal interplay in the SST of the study region (Figs. 2 and 3).

The coral reef health is often severely affected by the thermal stress, and mass bleaching is the common stress response of the coral community (Lough 2000). The observed massive bleaching affecting more than 60% of the live corals and the increase in the percentage contribution of dead corals in the reef ecosystem strongly indicates the profound impact of the El Niño 2015–2016 on the coral community of the Kavaratti atoll. The

Fig. 7 Species diversity (H') and species evenness of phytoplankton (J') along the sampling locations



report by the Department of Science and Technology (DST) of Lakshadweep, acknowledging a mass coral bleaching during March–April 2016 in conjunction with the El Niño 2015–2016 in this lagoon, supports our observation (http://intralak.nic.in/publish_LakTimes). The El Niño 2015–2016 induced mass bleaching in the Indonesian reef water and the Great Barrier Reef of the Pacific Ocean further signifies the global impact of this atmospheric event on the coral reef ecosystems (Normile 2016; Ampou et al. 2017). In Kavaratti atoll, during the strong El Niño of 1998, also almost all genera of the coral community were severely bleached (Arthur 2000; Arthur et al. 2006), which signifies the impact of this climate phenomenon on the reef ecosystem of the Indian Ocean. Hence, considering the persistent positive SST anomaly observed throughout the year in the Lakshadweep Sea region as a result of the El Niño 2015–2016, the severe bleaching seems to be a natural consequence contributing to a severe impact on the reef ecology.

In the present study, in addition to the marked variability observed in the SST and coral community in concurrence with the progression of the El Niño event, obvious changes were also observed in the chemical and other biological features of the reef waters. The variation

in the pH with relatively high values in the waning phase of El Niño indicates toward the changing chemistry of the reef waters in conjunction with the evolution of the climatic event. Though the coral reefs are critical in regulating oceanic CO₂ levels through their efficient atmospheric CO₂ absorption capacity, they may act as a potential CO₂ source depending on the temperature and aragonite saturation levels of the water column (Gray et al. 2012). As an elevation (reduction) in the surface water temperature decreases (increases) the dissolution of atmospheric CO₂ in ocean waters, the relatively warmer surface waters in the waning phase might have resulted in the reduced dissolution of CO₂, thus leading to the relatively high pH of the reef waters (Fushimi 1987).

In the marine ecosystem, the nutrient stoichiometry of the water column and in turn the bioavailability of the major nutrients plays a crucial role in shaping the abundance and community composition of the phytoplankton (Heil et al. 2007). In the present study, the lower nutrient concentration of reef waters during both the sampling periods substantiates the oligotrophic characteristic of the reef ecosystems. However, the substantial drop in the nutrient levels in the waning phase of the El Niño demanded a critical evaluation of the factors contributing to the changes in the nutrient dynamics of the Kavaratti reef waters (Fig. 4). The inputs from both new and regenerated production contribute toward the nutrient nourishment of the reef waters (Szmant-Froelich 1983). The input from river discharges also can be a potential nutrient source in reef ecosystems. However, as the Kavaratti atoll is lacking any river system, the nutrient supply through river discharges is unlikely. As rainfall and associated terrestrial runoff are considered to influence the nutrient nourishment of the reef community, their role in the nutrient dynamics of the Kavaratti reef water was also assessed. Being geographically located along the southeastern coast of the Indian subcontinent, the Lakshadweep Sea and associated coral islands come under the strong influence of the Indian

Table 3 Characterizing species of phytoplankton during peak and waning phases of El Niño

Species	Av.Abund	Av.Sim	Sim/ SD	Contrib%
Peak phase				
<i>Diploneis</i> sp.	3.12	8.82	0.84	29.50
<i>Prorocentrum lima</i>	3.84	7.72	0.88	25.82
Waning phase				
<i>Trichodesmium erythraeum</i>	4.39	17.61	2.99	42.00
<i>Navicula delicatula</i>	3.69	12.02	1.73	28.67
<i>Licmophora abbreviata</i>	2.05	3.96	0.69	9.44

Table 4 Discriminating species of phytoplankton between two phases

Species	Av.Abund	Av.Abund	Av.Diss	Diss/ SD	Contrib%
<i>Prorocentrum lima</i>	3.84	1.25	6.91	1.26	9.48
<i>Navicula delicatula</i>	1.85	3.69	6.04	1.34	8.29
<i>Trichodesmium erythraeum</i>	1.85	4.39	5.91	1.12	8.11
<i>Diploneis</i> sp.	3.12	1.30	5.88	1.17	8.06
<i>Thalassiosira</i> sp.	2.19	1.23	4.74	1.00	6.50
<i>Protoperdinium</i> sp.	1.91	1.06	4.37	0.93	5.99
<i>Licmophora abbreviata</i>	0.85	2.05	4.31	1.15	5.91
<i>Diplopsalis</i> sp.	1.85	0.57	3.76	0.89	5.16

summer monsoon. In general, the torrential precipitation in and around this region is mostly brought about by the summer monsoonal showers whose onset is generally from early June (Joseph et al. 1994). The present sampling was carried out during March–May, the spring intermonsoon period, characterized by marginal rainfall (88.6 mm) much lower than the amount of precipitation received during the summer monsoon period (858.4 mm

for the period of June–September 2015) (IMD 2016). Hence, the intermonsoonal scanty rainfall and associated runoff contributing to the nutrient status of the reef waters gets nullified. Advection of nutrient-rich oceanic waters is also considered as a primary nutrient source of reef waters (Zhang et al. 2011). However, the oligotrophic condition reported in the Lakshadweep Sea during the spring intermonsoon period (Sengupta et al. 1979) reduces the possibility of nutrient nourishment of reef waters through oceanic water advection. Moreover, lateral advection of nutrient-rich upwelled waters in concurrence with the mesoscale physical process like upwelling is also considered as an important process through which the reef ecosystems get nourished. In the northern Indian Ocean, upwelling usually occurs in conjunction with the summer monsoon (June–September) (Banse 1959). The period of the current sampling much before the onset of the southwest monsoon and upwelling further invalidates the influence of this mesoscale process in augmenting the nutrient conditions of the reef waters. Hence, the perpetual utilization of the available nutrients in the water column by the biotic community might have resulted in the significantly less nutrient concentration in the waning phase compared to the peak period of El Niño.

The size-structured phytoplankton biomass analysis helped in elucidating the interlink among the variability in the physical environment, nutrient stoichiometry, and the phytoplankton community in the present study. The predominance of the nanoplankton biomass over other phytoplankton size groups throughout the study indicates toward the low-nutrient environment prevailing in the reef waters. Nutrient-rich waters, characteristics of upwelling and cold core eddy regions, are often

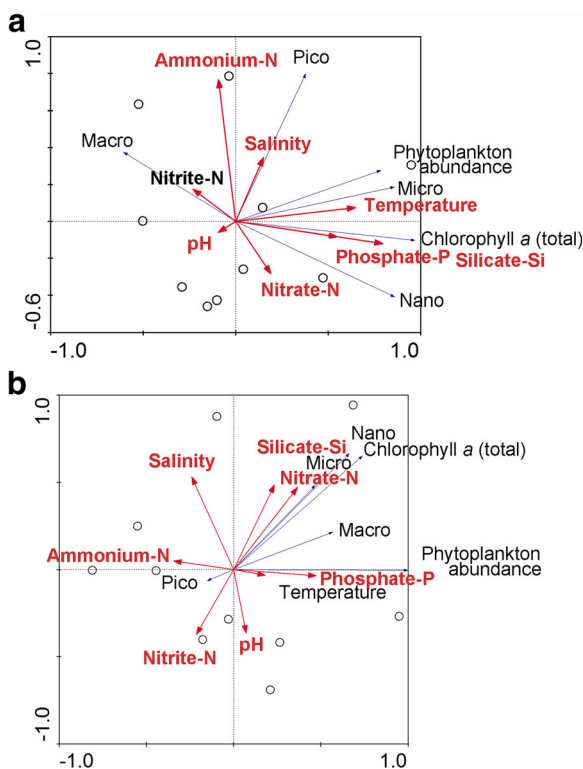


Fig. 8 RDA triplot showing interrelations between the abiotic and biotic components during **a** peak and **b** waning phases

predominated by large-sized phytoplankton community (Chisholm 1992). The competitive disadvantage faced by the larger phytoplankton under oligotrophic condition usually results in their replacement by smaller nanoplankton which is considered best in utilizing the low nutrient levels of oligotrophic waters (Sommer 2000). As the nutrient uptake sites are more concentrated in smaller surface areas, the nanoplankton with the higher surface area to volume ratio has significant contribution in the total phytoplankton biomass in the nutrient-deficient waters of the Arabian Sea (Garrison et al. 2000). However, the present observation differs from the reef environment of the Sesoko Island, Japan, where the picoplankton was reportedly dominated (Tada et al. 2003).

In oligotrophic regions, the nutrient stoichiometry of the water column often plays a major role in the size structure of the phytoplankton community (Sommer 2000). Two major picoplanktonic cyanobacteria, *Synechococcus* and *Prochlorococcus*, are known to contribute greatly toward primary production in the nutrient-impooverished regions, including reef ecosystems (Lindell and Post 1995). Though species-level analysis of the picoplankton was not carried out in the present study, these two species have been reported to dominate in the near reef region of the Arabian Sea (Mitbavkar and Anil 2011). These cyanobacteria exhibit a strong preference for ammonia-N over nitrate, and some strains are even reported to grow exclusively on ammonia-N as their chief nitrogen source (Rückert and Giani 2004). The positive interrelation observed between ammonia-N and the picophytoplankton community during both the sampling periods (Fig. 8) substantiates the significant role of ammonia-N in the picoplankton biomass of the study area. Interestingly, though relatively high ammonia-N was observed in the study region, a corresponding increase was not evident in the picoplankton biomass. Besides nitrogen, the concentration of phosphorus-P in oceanic waters also forms a major limiting factor determining the phytoplankton preponderance and community structure (Smith 1984). The study region evidenced a lower phosphate concentration during both the sampling periods with a marked drop in concentration in the waning phase. The synchronized observation of relatively lower picophytoplankton biomass in the waning phase with the lower phosphate concentration indicates toward the phosphate limitation on the proliferation of the picoplankton community. Similar to the picoplankton, the biomass of both

nanoplankton and microplankton was also strongly correlated with phosphate-P, which in turn suggests the regulatory role of phosphate in phytoplankton production in this reef ecosystem. In addition to phosphate, the nanoplankton and microplankton exhibited a positive relation with the concentration of silicate-Si in the study region. Diatoms form the dominant taxa contributing chiefly to the nanoplankton and microplankton size fraction in the tropical Indian waters (Garrison et al. 1998; Madhu et al. 2010). As diatoms have siliceous frustules as their cell wall material, silicate plays a vital role in their growth and proliferation (Yool and Tyrrell 2003). Hence, the conspicuous relation of silicate with the biomass of nanoplankton and microplankton during both the sampling periods can be thus validated (Fig. 8).

In the oligotrophic oceanic waters of tropical and subtropical regions, the cyanobacterium *T. erythraeum* plays a critical role in the atmospheric nitrogen fixation process and thus gains paramount importance in the oceanic nitrogen cycle (Capone et al. 2005). Though this filamentous colonial diazotroph was observed during both the sampling periods, a marked increase was noticed in their contribution to the total phytoplankton community from 2.4% in the peak phase to 33.2% during the waning phase, when the concentration of all the major nutrients was relatively lower (Fig. 4). Though the intense oligotrophic condition of the waning phase might not be favorable for the growth of the most of the phytoplankton species, the incident lower nitrate-N concentration (50% of the sampling locations $<0.1 \mu\text{M}$) might not have affected the proliferation of this diazotrophic cyanobacterium. When compared to the picophytoplankton diazotrophs which are mostly known to utilize the dissolved inorganic phosphorus (phosphate), *T. erythraeum* is considered well efficient in utilizing the dissolved organic phosphorus (DOP) also (Sohm and Capone 2006). Though DOP was not estimated in the present study, studies suggesting high DOP accumulation even in phosphorus-limited oceanic regions (<http://www.whoi.edu/page.do?pid=131276>) supports the possibility of the efficient DOP utilization by the *T. erythraeum* in the study region. As the size range of *T. erythraeum* was $>200 \mu\text{M}$ (Supplementary Fig. 2) and due to their colonial nature, the relatively high biomass of the macrophytoplankton in the waning phase and the evident positive relation with the phosphate presumably justifies *T. erythraeum* as the primary contributor of the macrophytoplankton biomass in the study region. Though the

macroplankton community represented by the *T. erythraeum* exhibited a positive relation with the dissolved inorganic phosphate in the RDA, it is inferred that the DOP pool might have also played an important part in their higher abundance. Warmer temperature ($>30\text{ }^{\circ}\text{C}$), well-lit environment, and scanty rainfall are often regarded as the other prominent factors influencing the higher preponderances of these diazotrophs in oceanic waters (Capone et al. 1997). Of these, SST greater than ($>30\text{ }^{\circ}\text{C}$) contributed to a higher abundance of *Trichodesmium* in the reef waters of the Port Blair Bay (Sahu et al. 2014). In the present study, the relatively warmer temperatures, well-lighted environment with less cloud cover and the reduced pre-monsoonal showers might have augmented their higher preponderance in the reef waters during the waning phase. The less competition from the other phytoplankton community during the waning phase might have also formed a major factor favoring their higher abundance.

The changes in the physical and chemical attributes of the reef waters in association with both the seasonal changes and the influence of El Niño thus had a significant effect on the community composition and the size-structured biomass of the phytoplankton community. The discrete existence of the sampling locations during peak and waning phases of El Niño in the NMDS plot signify the influence of this climatic event on the phytoplankton community structure. Furthermore, the result of the MVDISP algorithm helped to understand the variability in the phytoplankton community structure between the two phases. The higher homogeneity in the phytoplankton community structure in sampling locations during the waning phase resulted in less dispersion value compared to the peak phase. The low nutrient availability throughout the sampling locations might have led to a less variable community structure dominated by the diazotrophic *T. erythraeum*, capable of proliferating in the oligotrophic environment. Besides, the status of the reef corals is also known to have a profound influence on the abundance and community structure of the phytoplankton community of the reef ecosystem (McKinnon et al. 2007). Hence, in the severely bleached environment in the waning phase, the less efficient nutrient recycling by the reef corals might have resulted in a relatively homogenous phytoplankton community structure compared to the peak phase.

The distinctness in the characteristics of the phytoplankton community in the two phases of the El Niño

evidenced through the MVDISP algorithm was further reflected in the one-way ANOSIM analysis. The variation evidenced in the physical environment, changes in the water chemistry of the reef waters, and intern the altered coral status of the reef ecosystem resulted in the significantly distinguishable phytoplankton community between the two phases (global $R = 0.329$, $P = 0.002$). The El Niño induced changes in the phytoplankton composition, biomass, and community structure has been reported in reefs (Tada et al. 2003), signifying the imperative effect of this climate event on the reef ecology. Of the total 36 species of phytoplankton observed during the study, the varying abundance of the 8 discriminating species (identified through SIMPER analysis) played a vital role in the formation of the distinct community structure of the peak and waning phases. Interestingly, in spite of the prominent changes in the community structure, the species diversity and evenness between two phases exhibited insignificant variations. The nutrient availability and the nutrient stoichiometry have a determining role in shaping the size-structured phytoplankton community and type of production (new or regenerated), and this in turn further helps in utilizing the full spectrum of the available nutrients (Legendre and Rassoulzadegan 1995). However, in spite of the variability in the physicochemical attributes, the phytoplankton community was capable of retaining their diversity in the reef waters through varied community structure.

In conclusion, the El Niño 2015–2016 resulting in high SST in this reef ecosystem of the Indian Ocean had a significant impact on the reef corals resulting in their mass bleaching and mortality. The pronounced variability in the physical attributes of the reef waters exerted a profound influence on the water chemistry and biological scenario of the reef ecosystem. In general, an oligotrophic condition prevailed in the reef waters, which in turn resulted in less phytoplankton biomass and abundance. The complexities in size-structured biomass of the phytoplankton community contributed significantly in interlinking the variability in the environment generated by the altered physical and chemical attributes of the reef waters. The diazotrophic cyanobacterium, *T. erythraeum*, had a crucial role in the community dynamics during the intense nutrient-depleted waning phase. Their efficiency in fixing atmospheric nitrogen and also their capability in utilizing the dissolved organic phosphorus pool favored their higher proliferation in the reef waters during the waning phase of El Niño and

thus played a prominent role in the sustenance of the phytoplankton standing stock even during the intense nutrient-deficient conditions of the reef waters. The future studies should be focused on how the nutrient dynamics and reef ecology changes with the possible recovery of the reef corals after the El Niño retreat.

Acknowledgements This research program was supported by the Institutional project OLP 1210 of CSIR–National Institute of Oceanography. The first author is thankful to the Council of Scientific and Industrial Research for a post-doctoral fellowship (CSIR-RA). This is a CSIR-NIO contribution number 6137.

References

Ampou, E. E., Johan, O., Menkes, C. E., Niño, F., Birol, F., Ouillon, S., & Andréfouët, S. (2017). Coral mortality induced by the 2015–2016 El-Niño in Indonesia: the effect of rapid sea level fall. *Biogeosciences*, *14*(4), 817–826. <https://doi.org/10.5194/bg-14-817-2017>.

Arthur, R. (2000). Coral bleaching and mortality in three Indian reef regions during an El Niño Southern Oscillation event. *Current Science*, *79*(12), 1723–1729.

Arthur, R., Done, T. J., Marsh, H., & Harriott, V. (2006). Local processes strongly influence postbleaching benthic recovery in the Lakshadweep Islands. *Coral Reefs*, *25*(3), 427–440.

Baker, A. C., Glynn, P. W., & Riegl, B. (2008). Climate change and coral reef bleaching: an ecological assessment of long-term impacts, recovery trends and future outlook. *Estuarine Coastal and Shelf Science*, *80*(4), 435–471.

Banse, K. (1959). On upwelling and bottom trawling off the southwest coast of India. *Journal of Marine Biology Association India*, *1*, 33–49.

Bell, P. R., & Elmetri, I. (1995). Ecological indicators of large-scale eutrophication in the Great Barrier Reef lagoon. *Oceanographic Literature Review*, *12*(42), 1145.

Canale, R. P., & Vogel, A. H. (1974). Effects of temperature on phytoplankton growth. *Journal of Sanitary Engineering Division*, *100*(1), 231–241.

Capone, D. G., Zehr, J. P., Paerl, H. W., Bergman, B., & Carpenter, E. J. (1997). *Trichodesmium*, a globally significant marine cyanobacterium. *Science*, *276*(5316), 1221–1229. <https://doi.org/10.1126/science.276.5316.1221>.

Capone, D. G., Burns, J. A., Montoya, J. P., Subramaniam, A., Mahaffey, C., Gunderson, T., Michaels, A. F., & Carpenter, E. J. (2005). Nitrogen fixation by *Trichodesmium* spp.: an important source of new nitrogen to the tropical and subtropical North Atlantic Ocean. *Global Biogeochemical Cycles*, *19*(2). <https://doi.org/10.1029/2004GB002331>.

Carte, B. K. (1996). Biomedical potential of marine natural products: marine organisms are yielding novel molecules for use in basic research and medical applications. *Bioscience*, *46*, 271–286.

Chen, S., Wu, R., Chen, W., Yu, B., & Cao, X. (2016). Genesis of westerly wind bursts over the equatorial western Pacific during the onset of the strong 2015–2016 El Niño.

Atmospheric Science Letters, *17*(7), 384–391. <https://doi.org/10.1002/asl.669>.

Chisholm, S. W. (1992). Phytoplankton size. In P. G. Falkowski & A. G. Woodhead (Eds.), *Primary productivity and biogeochemical cycles in the sea* (pp. 213–237). New York: Plenum Press.

Cinner, J. E., McClanahan, T. R., MacNeil, M. A., Graham, N. A. J., Daw, T. M., Mukminin, A., Feary, D. A., Rabearisoa, A. L., Wamukota, A., Jiddawi, N., Campbell, S. J., Baird, A. H., Januchowski-Hartley, F. A., Hamed, S., Lahari, R., Morove, T., & Kuange, J. (2012). Comanagement of coral reef social-ecological systems. *Proceedings of the National Academy of Sciences*, *109*(14), 5219–5222. <https://doi.org/10.1073/pnas.1121215109>.

Clarke, K. R., & Gorley, R. N. (2015). *PRIMER v7: user manual/tutorial*. Plymouth: PRIMER-E.

English, S., Wilkinson, C., & Baker, V. (1997). *Survey manual for tropical marine resources*. Townsville: Australian Institute of Marine Science.

Furnas, M. (2007). Intra-seasonal and inter-annual variations in phytoplankton biomass, primary production and bacterial production at North West Cape, Western Australia: links to the 1997–1998 El Niño event. *Continental Shelf Research*, *27*(7), 958–980. <https://doi.org/10.1016/j.csr.2007.01.002>.

Fushimi, K. (1987). Variation of carbon dioxide partial pressure in the western North Pacific surface water during the 1982/83 El Niño event. *Tellus B*, *39*(1–2), 214–227. <https://doi.org/10.3402/tellusb.v39i1-2.15339>.

Gadgil, S., & Francis, P. A. (2016). El Niño and the Indian rainfall in June. *Current Science*, *110*, 1010–1022.

Garate-Lizarraga, I., & Beltrones, D. A. S. (1998). Time variation in phytoplankton assemblages in a subtropical lagoon system after the 1982–1983 “El Niño” event (1984 to 1986). *Pacific Science*, *52*(1), 79–97.

Garrison, D. L., Gowing, M. M., & Hughes, M. P. (1998). Nano- and microplankton in the northern Arabian Sea during the Southwest monsoon, August–September 1995: a US–JGOFS study. *Deep Sea Research II*, *45*(10–11), 2269–2299. [https://doi.org/10.1016/S0967-0645\(98\)00071-X](https://doi.org/10.1016/S0967-0645(98)00071-X).

Garrison, D. L., Gowing, M. M., Hughes, M. P., Campbell, L., Caron, D. A., Dennett, M. R., Shalapyonok, A., Olson, R. J., Landry, M. R., Brown, S. L., & Liu, H. B. (2000). Microbial food web structure in the Arabian Sea: a US JGOFS study. *Deep Sea Research II*, *47*(7), 1387–1422. [https://doi.org/10.1016/S0967-0645\(99\)00148-4](https://doi.org/10.1016/S0967-0645(99)00148-4).

Gray, S. E., DeGrandpre, M. D., Langdon, C., & Corredor, J. E. (2012). Short-term and seasonal pH, pCO₂ and saturation state variability in a coral-reef ecosystem. *Global Biogeochemical Cycles*, *26*(3), GB3012. <https://doi.org/10.1029/2011GB004114>.

Guildford, S. J., & Hecky, R. E. (2000). Total nitrogen, total phosphorus, and nutrient limitation in lakes and oceans: is there a common relationship? *Limnology and Oceanography*, *45*(6), 1213–1223. <https://doi.org/10.4319/lo.2000.45.6.1213>.

Heil, C. A., Revilla, M., Glibert, P. M., & Murasko, S. (2007). Nutrient quality drives differential phytoplankton community composition on the southwest Florida shelf. *Limnology and Oceanography*, *52*(3), 1067–1078. <https://doi.org/10.4319/lo.2007.52.3.1067>.

- Hughes, T. P., Baird, A. H., Bellwood, D. R., Card, M., Connolly, S. R., Folke, C., Grosberg, R., Hoegh-Guldberg, O., Jackson, J. B., Kleypas, J., Lough, J. M., Marshall, P., Nyström, M., Palumbi, S. R., Pandolfi, J. M., Rosen, B., & Roughgarden, J. (2003). Climate change, human impacts, and the resilience of coral reefs. *Science*, *301*(5635), 929–933. <https://doi.org/10.1126/science.1085046>.
- IMD (2016). <http://www.imd.gov.in>. Accessed 2016.
- James, P. S. B. R. (2011). The Lakshadweep: islands of ecological fragility, environmental sensitivity and anthropogenic vulnerability. *Journal of Coastal Environment*, *2*(1), 9–25.
- Joseph, P. V., Eischeid, J. K., & Pyle, R. J. (1994). Interannual variability of the onset of the Indian summer monsoon and its association with atmospheric features, El Niño, and sea surface temperature anomalies. *Journal of Climate*, *7*(1), 81–105. [https://doi.org/10.1175/1520-0442\(1994\)007<0081:IVOTOO>2.0.CO;2](https://doi.org/10.1175/1520-0442(1994)007<0081:IVOTOO>2.0.CO;2).
- Kelley, R. (2009). Indo Pacific coral finder. See www.byoguides.com.
- Legendre, L., & Rassoulzadegan, F. (1995). Plankton and nutrient dynamics in marine waters. *Ophelia*, *41*(1), 153–172. <https://doi.org/10.1080/00785236.1995.10422042>.
- Lindell, D., & Post, A. F. (1995). Ultraphytoplankton succession is triggered by deep winter mixing in the Gulf of Aqaba (Eilat), Red Sea. *Limnology and Oceanography*, *40*(6), 1130–1141. <https://doi.org/10.4319/lo.1995.40.6.1130>.
- Lough, J. M. (2000). 1997–98: Unprecedented thermal stress to coral reefs? *Geophysical Research Letters*, *27*(23), 3901–3904. <https://doi.org/10.1029/2000GL011715>.
- Madhu, N. V., Balachandran, K. K., Martin, G. D., Jyothibabu, R., Thottathil, S. D., Nair, M., Joseph, T., & Kusum, K. K. (2010). Short-term variability of water quality and its implications on phytoplankton production in a tropical estuary (Cochin backwaters—India). *Environmental Monitoring and Assessment*, *170*(1–4), 287–300. <https://doi.org/10.1007/s10661-009-1232-y>.
- Maranon, E., Cermenno, P., Latasa, M., & Tardonléké, R. D. (2012). Temperature, resources, and phytoplankton size structure in the ocean. *Limnology and Oceanography*, *57*(5), 1266–1278. <https://doi.org/10.4319/lo.2012.57.5.1266>.
- McKinnon, A. D., Richardson, A. J., Burford, M. A., & Furnas, M. J. (2007). Vulnerability of Great Barrier Reef plankton to climate change. In J. E. Johnson & P. A. Marshall (Eds.), *Climate change and the Great Barrier Reef* (pp. 122–152). Australia: Great Barrier Reef Marine Park authority and Australian Greenhouse office.
- McPhaden, M. J., Zebiak, S. E., & Glantz, M. H. (2006). ENSO as an integrating concept in Earth science. *Science*, *314*(5806), 1740–1745. <https://doi.org/10.1126/science.1132588>.
- Mitbavkar, S., & Anil, A. C. (2011). Tiniest primary producers in the marine environment: an appraisal from the context of waters around India. *Current Science*, *100*(7), 986–988.
- Normile, D. (2016). El Niño's warmth devastating reefs worldwide. *Science*, *352*(6281), 15–16. <https://doi.org/10.1126/science.352.6281.15>.
- Pillai, C. S. G. (1996). Coral reefs of India, their conservation and management. In N. G. Menon & C. S. G. Pillai (Eds.), *Marine Biodiversity Conservation and Management*. Cochín: ICAR.
- Pillai, C. S. G., & Jasmine, S. (1989). The coral fauna of Lakshadweep. *CMFRI Bulletin*, *43*, 179–195.
- Racault, M. F., Raitsos, D. E., Berumen, M. L., Brewin, R. J., Platt, T., Sathyendranath, S., & Hoteit, I. (2015). Phytoplankton phenology indices in coral reef ecosystems: application to ocean-color observations in the Red Sea. *Remote Sensing of Environment*, *160*, 222–234. <https://doi.org/10.1016/j.rse.2015.01.019>.
- Roxy, M., Gualdi, S., Drbohlav, H. K. L., & Navarra, A. (2011). Seasonality in the relationship between El Niño and Indian Ocean dipole. *Climate Dynamics*, *37*(1–2), 221–236. <https://doi.org/10.1007/s00382-010-0876-1>.
- Rückert, G. V., & Giani, A. (2004). Effect of nitrate and ammonium on the growth and protein concentration of *Microcystis viridis* Lemmermann (Cyanobacteria). *Brazilian Journal of Botany*, *27*, 325–331.
- Sahu, B. K., Begum, M., Kumarasamy, P., Vinithkumar, N. V., & Kirubakaran, R. (2014). Dominance of *Trichodesmium* and associated biological and physico-chemical parameters in coastal waters of Port Blair, South Andaman Island. *Indian Journal of Geo-Marine Sciences*, *43*, 1–7.
- SenGupta, R., Mores, C., Kureishy, T. W., Sankaranarayanan, V. N., Jana, T. K., Naqvi, S. W. A., & Rajagopal, M. D. (1979). Chemical oceanography of the Arabian Sea: part IV—Laccadive Sea. *Indian Journal of Geo-Marine Sciences*, *8*, 215–221.
- Shenoi, S. S. C., Shankar, D., & Shetye, S. R. (1999). On the sea surface temperature high in the Lakshadweep Sea before the onset of the southwest monsoon. *Journal of Geophysical Research Oceans*, *104*(C7), 15703–15712. <https://doi.org/10.1029/1998JC900080>.
- Smith, S. V. (1984). Phosphorus versus nitrogen limitation in the marine environment. *Limnology and Oceanography*, *29*(6), 1149–1160. <https://doi.org/10.4319/lo.1984.29.6.1149>.
- Sohm, J. A., & Capone, D. G. (2006). Phosphorus dynamics of the tropical and subtropical north Atlantic: *Trichodesmium* spp. versus bulk plankton. *Marine Ecology Progress Series*, *317*, 21–28. <https://doi.org/10.3354/meps317021>.
- Sommer, U. (2000). Scarcity of medium-sized phytoplankton in the northern Red Sea explained by strong bottom-up and weak top-down control. *Marine Ecology Progress Series*, *197*, 19–25. <https://doi.org/10.3354/meps197019>.
- Spalding, M. D., Ravilious, C., & Green, E. P. (2001). *World atlas of coral reefs*. Berkeley: University of California Press.
- Stramma, L., Fischer, T., Grundle, D. S., Krahnemann, G., Bange, H. W., & Marandino, C. A. (2016). Observed El Niño conditions in the eastern tropical Pacific in October 2015. *Ocean Science*, *12*(4), 861–873. <https://doi.org/10.5194/os-12-861-2016>.
- Suresh, V. R., & Mathew, K. J. (1999). Studies on phytoplankton productivity in Kavaratti atoll, Lakshadweep. *Indian Journal of Fisheries*, *46*(4), 401–403.
- Szmant-Froelich, A. S. (1983). Functional aspects of nutrient cycling on coral reefs. In M. L. Reaka (Ed.), *The ecology of deep shallow coral reefs* (pp. 133–139). Pennsylvania: Forgotten Books.
- Tada, K., Sakai, K., Nakano, Y., Takemura, A., & Montani, S. (2003). Size-fractionated phytoplankton biomass in coral reef waters off Sesoko Island, Okinawa, Japan. *Journal of Plankton Research*, *25*(8), 991–997. <https://doi.org/10.1093/plankt/25.8.991>.
- Tomas, C. R. (1997). *Identifying marine phytoplankton*. New York: Academic.

- Utermöhl, H. (1931). Neue Wege in der quantitativen Erfassung des Planktons (mit besonderer Berücksichtigung des Ultraplanktons). *Verhandlungen der Internationalen Vereinigung für Theoretische und Angewandte Limnologie*, 5, 567–596
- Venkataraman, K. (2011). Coral reefs of India. In D. Hopley (Ed.), *Encyclopedia of modern coral reefs, structure, form and process* (pp. 267–275). Netherland: Springer. https://doi.org/10.1007/978-90-481-2639-2_64.
- Yool, A., & Tyrrell, T. (2003). Role of diatoms in regulating the ocean's silicon cycle. *Global Biogeochemical Cycles*, 17(4). <https://doi.org/10.1029/2002GB002018>.
- Zhang, Z., Lowe, R., Falter, J., & Ivey, G. (2011). A numerical model of wave-and current-driven nutrient uptake by coral reef communities. *Ecological Modelling*, 222(8), 1456–1470. <https://doi.org/10.1016/j.ecolmodel.2011.01.014>.